THE AMERICAN SOCIETY OF MECHANICAL ENGINEERS
345 E. 47th St., New York, N.Y. 10017

95-GT-193

A SEMI-EMPIRICAL THEORY FOR SURFACE MOUNTED AERODYNAMIC WALL SHEAR STRESS GAUGES

Mark R. D. Davies and James T. Duffy
Department of Mechanical and Aeronautical Engineering
University of Limerick
Limerick
Ireland

ABSTRACT

A new semi-empirical theory relating aerodynamic wall shear stress to the mean voltage from a surface mounted constant temperature hot film gauge is presented. High spatial resolution thermal images of the sensor area are used to obtain values for the mean sensor temperature and the thermal dimensions of the sensor. These thermal dimensions are shown to be invariant with Reynolds number. This data is used in the derivation of a new theory that effectively decouples the convection and conduction and hence removes the need for a fully conjugate analysis. The correct form of the relationship between sensor voltage and wall shear stress is a necessary prerequisite for gauge calibration and hence the quantification of aerodynamic wall shear stress. A calibration methodology is presented in an accompanying paper.

NOMENCLATURE

a,b	First and second calibration constants	—
C_p	Specific heat at constant pressure	KJ/Kg K
d	Distance	m
dp/dx	Pressure gradient	N/m^3
dq	Heat transfer per unit area	W/m^2
dQ	Heat transfer	W
dx	Small distance in x direction	m
H	Thickness of substrate	m
i	Current	A
K	Thermal conductivity	W / m K
L	Sensor length	m
N_{ul}	Nusselt number = $(V_s^2-V_o^2)/(R_hWK_f(T_s-T_\infty))$	—
Pr	Prandtl number	—
Q_T	Total Convective heat transfer	W
R_h	Hot Sensor Resistance	Ω
Re	Reynolds number	—
T	Temperature	K
U	Velocity	m/s
V	Voltage	V
W	Sensor width	m
x,y,z	Cartesian coordinates	m
Greek		
δ	Boundary-layer thickness	m
η	y/δ_t	—
λ	Temperature shape parameter	—
μ	Dynamic viscosity	Kg/ms
ρ	Density	Kg/m^3
τ_w	Wall shear stress	N/m^2
Suffices		
act	Actual	
b	Fluid temperature in thermal boundary-layer	
eff	Effective	
f	Fluid	
L	Mean temperature over thermal length	
max	Maximum temperature for the x direction profile	
s	Sensor	
TA	Mean temperature of the thermal area	
Th	Thermal length	
Th′	To the point of interest along the thermal length	
x,y	x and y Directions	
1,2	Substrate 1, Substrate 2	
∞,0	Free-stream and zero flow conditions	

INTRODUCTION

Since the 1960's thin film surface mounted gauges, operating at a constant temperature, have been used to investigate aerodynamic shear stress. All such gauges need calibrating before they can be used to quantify this stress and consequently they have not generally been used for quantitative work. They have instead found many applications

Presented at the International Gas Turbine and Aeroengine Congress and Exposition
Houston, Texas - June 5-8, 1995

on isolated aerofoils and turbomachine blade rows in finding the position of boundary layer transition, Hodson (1985) and Schroeder (1989), usually by the qualitative interpretation of the real time gauge signal. However, the need has not gone away for an experimental method of finding the aerodynamic shear stress and surface mounted gauges offer many advantages over other methods such as surface pitot tubes. Measurements of this stress gives an insight into drag and loss mechanisms and a virtually non-intrusive measurement of a significant boundary-layer parameter for comparison with computational predictions.

The first requirement for the calibration of a shear stress gauge is a theory linking the sensor voltage to the shear stress and this issue is addressed in this paper. The aim here is to produce a calibrating equation so that subsequent calibrating experiments can be used to find the unknown parameters. As will be shown it is not expected that this calibration will work for all sensor geometries and overheat temperatures. What is shown is that a semi-empirical method, relying on a known surface temperature distribution, can be used for a given gauge and substrate at a particular overheat temperature.

The new theory developed is for a Dantec 55R47 glue on gauge connected to a constant temperature anemometer (CTA), mounted on a relatively large aluminium surface. The purpose of the CTA circuit is to keep the sensor resistance and hence the sensor temperature constant with varying air flow. A review of hot film anemometry is given by Lomas (1986). The Dantec 55R47 gauge consists of nickel film deposited on a kapton (polyimide) substrate and covered with a quartz coating. As it may be considered a thin film, with a thickness of approximately 1μm, film edge heat transfer is ignored and theories based on convection to the fluid and conduction into the substrate are sufficient. Radiation is neglected as it contributes less than 0.5% of the power dissipated at zero flow.

Several theories exist where the wall shear stress is related to the convective heat transfer for steady flow, Bellhouse and Schultz (1966) and Brown (1967), and for unsteady flow, Menendez and Ramaprian (1985). However, there are questions as to the correctness of some assumptions made in the development of these theories and also uncertainty over the values of some constants contained in them. These problems limit their usefulness when it comes to the quantification of wall shear stress on arbitrary shapes. Curle (1961) first presented the relationship, given by equation (1), developed from

$$\frac{d}{dx}\left[\frac{\underline{a}\tau_w K_f^2(T_s-T_\infty)^3}{dq^2} - \frac{\left(\frac{dp}{dx}\right)\underline{b}K_f^3(T_s-T_\infty)^4}{2\,dq^3}\right] = \frac{-\mu^2 dq}{\rho K_f Pr} \quad (1)$$

$$\underline{\lambda} = \frac{dq\,\delta_t}{K_f(T_s-T_\infty)} \; ; \; \underline{a} = \underline{\lambda}^2\int_0^1 \eta f(\eta)d\eta \; ; \; \underline{b} = -\underline{\lambda}^3\int_0^1 \eta^2 f(\eta)d\eta$$

the thermal energy integral equation, which is the basis for many theories. The values of wall shear stress, fluid properties, and equation constants a and b, were assumed to be constant over the sensor length. However, nothing was known of the streamwise variation in surface to fluid temperature difference or heat transfer coefficient, so the equation could not be solved.

To solve equation (1) Bellhouse and Schultz (1966) used an assumption that the temperature difference and the convective heat transfer were constant over the sensor length. Mathews (1985) pointed out, that if both of these quantities are constant over the sensor then the differential on the left hand side of equation (1) equals zero and the equation does not describe the flow over the sensor. It will be shown that there is in fact a very significant variation of surface temperature over the sensor, although the heat transfer coefficient is approximately constant when the sensor is mounted on substrates with large thermal conductivities.

Following the assumptions of Bellhouse and Schultz (1966), equation (1) may be manipulated to give a relationship between wall shear stress and convective heat transfer from the sensor:

$$\left[\frac{\rho Pr}{\mu^2}\right]^{1/3} W L^{\frac{2}{3}} K_f (T_s-T_\infty)\left[\underline{a}\,\tau_w - \frac{dp}{dx}\frac{\underline{b}\,L}{2\,N_{ul}}\right]^{1/3} = Q_T \quad (2)$$

There are further problems encountered when equation (2) is used. Firstly, the values of the constants a and b are unknown and must be obtained by similarity approximations, Liepmann (1958), or empirically, Curle (1961) or numerically, Menendez and Ramaprian (1985). Secondly, the sensor dimensions are present in equation (2) but no account is taken of heat spread around the sensor. This problem is addressed herein.

For flows with no pressure gradient, equation (2) gives the standard relationship between V_s^2 and $\tau_w^{1/3}$:

$$V_s^2 = A\tau_w^{1/3} + V_0^2$$

$$A = \left[\frac{\rho Pr}{\mu^2}\right]^{1/3} W L^{2/3} K_f R_h (T_s-T_\infty)\,\underline{a}^{1/3} \quad (3)$$

The sensor voltage squared is related to the power dissipated by the sensor. Parameter A is associated with the forced convection losses and may be considered as a measure of flow sensitivity and is found experimentally to be invariant with local Reynolds number (Duffy *et al* 1995). As all parameters other than the sensor area, are known or assumed to be constant, it indirectly implies that the thermal area remains constant with increasing local Reynolds number. Although this would appear to be a reasonable assumption to make, indeed Menendez and Ramaprian (1985) have done so in extending their theory to unsteady flow, there are no experimental results to directly substantiate it. V_0^2 is assumed to represent the conductive heat loss to the substrate. The measured value is not the same as the value found by plotting experimental data in the form of equation (3) as reported by Mathews (1985). This problem is discussed by Duffy *et al* (1995)

who address gauge calibration.

The measurement of wall shear stress in flows with no pressure gradients are not of the greatest interest. Therefore equation (4):

$$V_s^2 = A\left[\tau_w - \frac{dp}{dx}\frac{b\,L}{2\,a\,N_{ul}}\right]^{1/3} + V_0^2 \qquad (4)$$

which introduces the pressure gradient into the relationship is required and consequently the second unknown, parameter b, is introduced.

Despite these reservations there has been a considerable amount of experimental work, in zero pressure gradients by Bellhouse and Schultz (1966), Pope (1972), and Brown (1967) and in flows with pressure gradients by Bellhouse and Schultz (1966), that verify the form of relationships given in equations (3) and (4) respectively. To precede with gauge calibration it is necessary to break equation (4) into its individual parameters and to quantify each so that the constants a and b may be found experimentally. If this were not possible then experiments, varying the shear stress and pressure gradient independently, could be used for calibration, but no physical meaning could then be assigned to the calibrating constants.

The approach taken in this paper is to use high spatial resolution radiation thermography to obtain the sensor temperature distribution and hence its effective dimensions. This is then used as a boundary condition in the solution of equation (1), both removing the need to assume constant temperature over the sensor, and for a fully conjugate solution. The heat transfer coefficient is still assumed spatially constant and evidence from conjugate solutions are used to support this. Duffy *et al* (1995) have evaluated the unknown parameters for flows with free-stream pressure gradients and used calibrated gauges to measure the aerodynamic wall shear stress on a two dimensional turbine blade.

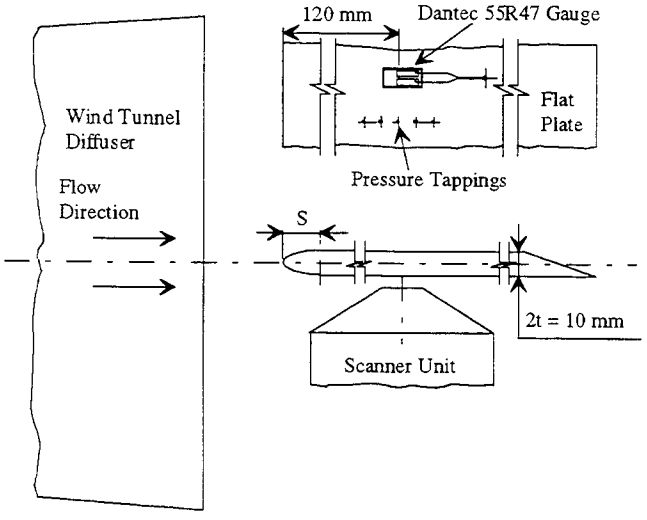

FIG. 1 FLAT PLATE AND SCANNER UNIT

EXPERIMENTAL SET UP

The Dantec 55R47 gauge, operated at an overheat of 383 K above a reference air temperature of 293 K, was mounted on an aluminium flat plate designed with an elliptical leading edge ratio of the semimajor axis to half the plate thickness, s/t, equal to 3, based on work by Davis (1980), to prevent leading edge separation. The plate was mounted in the jet of a low velocity atmospheric wind tunnel, see Fig. 1.

THERMAL IMAGING

An Agema Thermovision 880 infrared scanning system comprised of, a scanner unit, control unit CU 800 V, and a COMPAQ 286 PC, was used to analyse the surface temperature of a Dantec 55R47 hot-film gauge. The scanner unit was fitted with a microscope lens which had a temperature resolution of 0.7 K with an accuracy of ± 0.72% at 333 K. The lens had a field of view of 2.56 mm^2 giving a spatial resolution of 11 μm. This allowed the detection of the surface temperature variations across the sensor with high spatial resolution which is very important considering the size of the sensor, see Fig. 2.

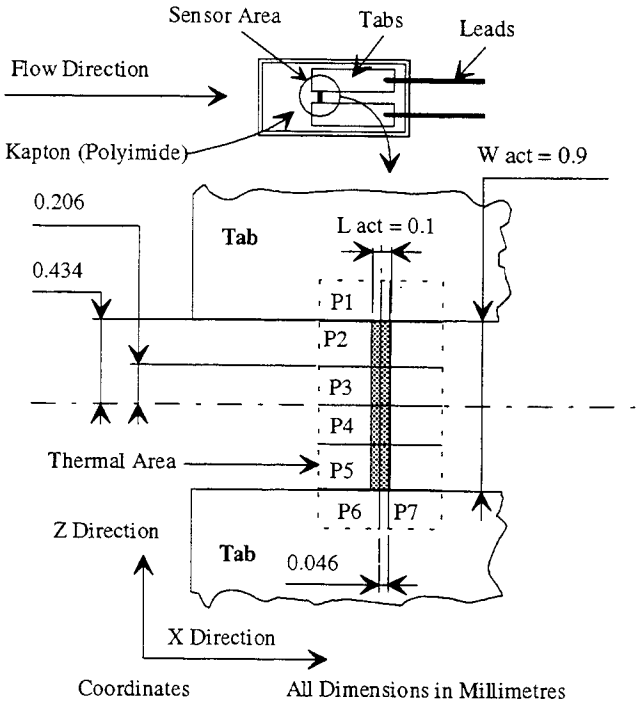

FIG. 2 DANTEC 55R47 GAUGE SHOWING THE EXPERIMENTAL TEMPERATURE PROFILE POSITIONS P1 TO P7 ON THE SENSOR AREA

Although thermal imaging is a non-contact operation the microscope lens has a focal length of only four millimetres. To ensure that the scanner lens did not interfere with the flow a number of test

runs were performed with and without the scanner unit in place. Plots of sensor voltage versus local Reynolds number, shown in Fig. 3, provide a sufficient indication that the interference effect was negligible.

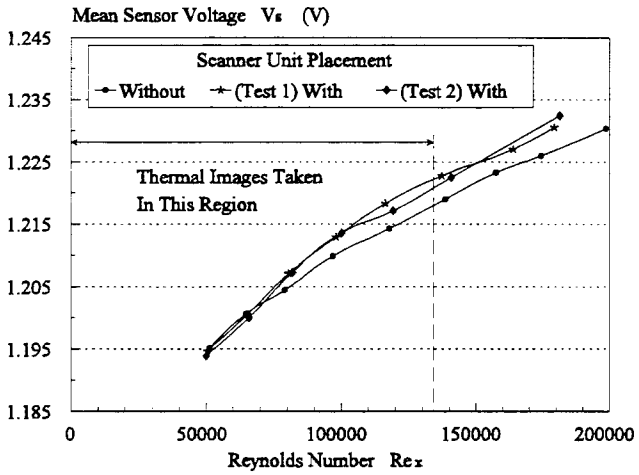

FIG. 3 SCANNER UNIT EFFECT

To determine the invariance of the thermal area around the sensor with local Reynolds number, thermal images were taken in the range, $0<Re_x<1.33x10^5$. Extension of the analysis to higher velocities was not possible due to vibration of the scanner unit. Fig. 4 indicates that the thermal dimensions of the sensor are invariant with Reynolds number.

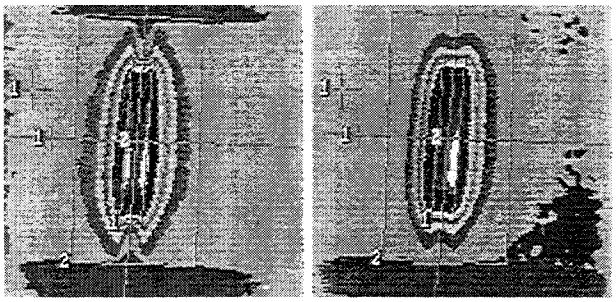

(a) $Re_x = 0$ (b) $Re_x = 1.33x10^5$

FIG. 4 THERMAL IMAGES, FLOW FROM LEFT TO RIGHT, EMISSIVITY = 1

An emissivity of 1 was assigned to the surface because of the inability of the analysis software to handle the number of different emissivities of the different materials making up the gauge. Therefore it should be noted that the temperatures indicated by these thermal images are incorrect but this does not effect the conclusion drawn above. The values of the mean temperature over the thermal area, obtained from the images, Fig. 4, taken with varying local Reynolds number, are plotted in Fig. 5. The percentage variation of the mean temperature over the thermal area about its mean was found to be ±0.85%. This is largely explained by the accuracy of the lens.

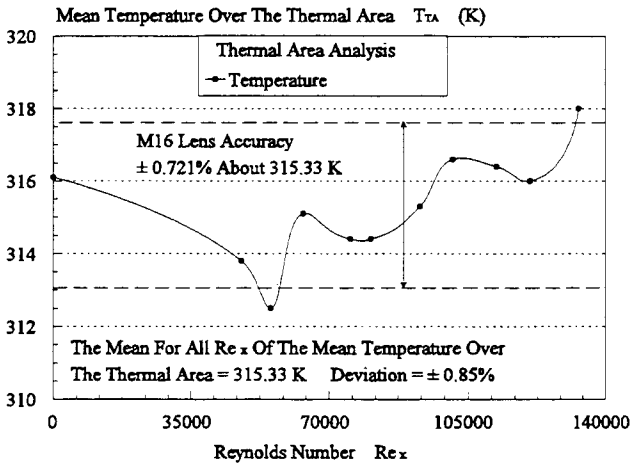

FIG. 5 THERMAL IMAGE EXPERIMENTAL RESULTS

Temperature Profiles And Thermal Area

To obtain correct temperature profiles the sensor area had to be coated with a material of known emissivity, in this case black paint, giving an emissivity value of approximately unity. The software was used to check the accuracy of this by area averaging the sensor temperature. This gave a sensor temperature of 401 K, see Fig. 6, compared to a mean sensor temperature of 403 K set by choosing the appropriate hot sensor resistance to balance the CTA bridge. This verifies that the blackened gauge is at the correct temperature. The sensor overheat temperature was set to the highest allowable value to give maximum sensor sensitivity (Lomas, 1986).

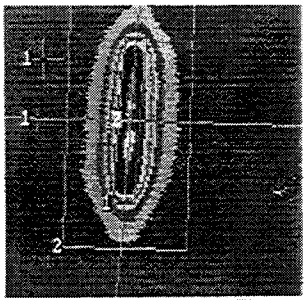

FIG. 6 THERMAL IMAGE OF BLACK COATED SENSOR ZERO FLOW, T_{TA}= 324.4 K, T_S= 401 K, EMISSIVITY= 1

Temperature profiles were taken at five sections in the x direction and two sections in the z direction as defined in Fig. 2. These are shown in Figs. 7 and 8. The gauge thermal area is defined by the line where the thermal gradient is zero. This is at ±28 and ±57 pixels in Figs. 7 and 8 respectively. Following this definition the thermal dimensions, L_{Th} x W_{Th}, are 0.65 mm x 1.31 mm, in comparison to 0.1 mm x 0.9 mm for the sensor metal dimensions.

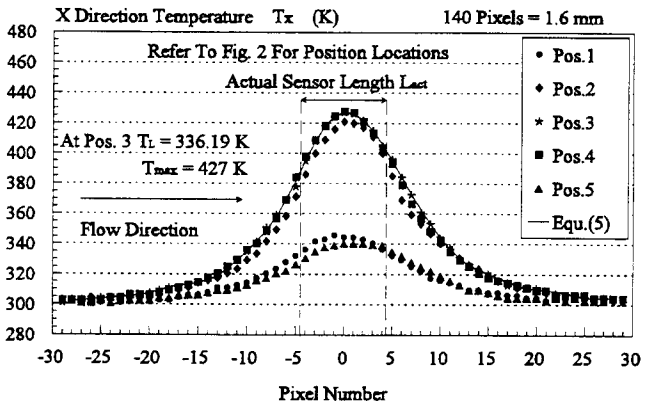

FIG. 7 X DIRECTION TEMPERATURE PROFILE

Curve Fit Of The Temperature Profiles. To enable the experimental temperature profile data to be used in the development of the new theory the temperature profiles at positions 3 and 6, see Fig. 2, were curve fitted using a Fourier series. The general form of the curve fit is given in equation (5), which can be applied to either direction by substituting the appropriate values.

$$T_x \text{ or } T_z = a_0 + a_1 Cos\left(\frac{\pi d'_{Th}}{d_{Th}}\right) + a_2 Cos\left(\frac{2\pi d'_{Th}}{d_{Th}}\right) + \ldots + a_n Cos\left(\frac{n\pi d'_{Th}}{d_{Th}}\right) \quad (5)$$

The variables d_{Th} and d'_{Th} in equation (5), are the thermal length and the distance to the point of interest measured from the edge of the thermal area respectively. The equation coefficients and the thermal lengths for both directions are given in Table 1. Comparison of the curve fits, for the x and z directions, with experimental data are given in Figs. 7 and 8.

Integration of equation (5) gives the mean temperature over the sensor thermal length where the appropriate values of the coefficients and the numbers of terms, m, for the x and z directions, are chosen from Table 1. Equation (6) gives the integral for the x direction but the equation form is exactly the same for the z direction and can be obtained by substituting the appropriate values.

$$\left[2\int_0^{\frac{d_{Th}}{2}} T_x\, dx\right]\left[\frac{1}{d_{Th}}\right] = a_0 + \sum_{n=1}^{n=m} \frac{a_{2n-1}}{2n-1}\left(\frac{2}{\pi}\right)(-1)^{n+1} = T_L \quad (6)$$

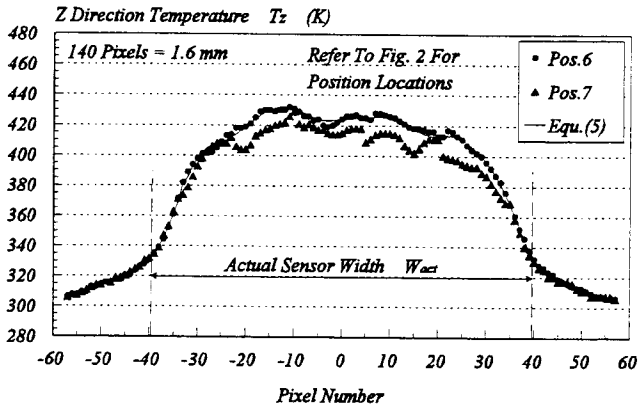

FIG. 8 Z DIRECTION TEMPERATURE PROFILES

TABLE 1 COEFFICIENTS FOR EQUATIONS (5) AND (6)

a_n	x Direction	z Direction
a_0	339.1368	378.0696
a_1	-002.99437	000.59619
a_2	-051.03279	-064.57404
a_3	003.59448	-001.26771
a_4	022.67281	-014.84869
a_5	-002.09791	002.30796
a_6	-009.82153	005.77572
a_7	000.69924	000.03539
a_8	003.11049	004.79954
a_9	000.01227	-001.15428
a_{10}	-001.00563	001.28302
a_{11}	-000.16796	000.56560
a_{12}	000.48610	-004.06787
a_{13}	000.52962	-001.09321
a_{14}	-000.33533	-001.49434
a_{15}	-000.56442	000.52768
a_{16}	-000.18523	000.45599
a_{17}	-000.23873	000.95049
a_{18}	000.41647	000.18162
a_{19}		-000.34637
a_{20}		000.46905
a_{21}		-000.733
a_{22}		-000.29499

x Direction:- $d_{Th} = L_{Th}$ = 0.6514285 mm ; m = 9
z Direction:- $d_{Th} = W_{Th}$ = 1.3142857 mm ; m = 11
For both directions:- $0 \le d'_{Th} \le d_{Th}$

CALCULATION OF EFFECTIVE AREA

By inspection of Figs. 2,7 and 8, it can be seen that the x direction temperature profile is not constant over all of the sensor thermal width

due to end effects. Therefore, the assumption that the x direction temperature profile at position 3, see Fig. 2, is representative of the streamwise variation in temperature across the entire thermal width of the sensor is incorrect. A heat balance is therefore used to define the effective width, W_{eff}, which is used as the width dimension for heat transfer in the subsequent analysis.

$$W_{eff} = W_{Th}\left[\frac{T_{TA} - T_\infty}{T_L - T_\infty}\right] \tag{7}$$

The convective heat transfer is therefore modelled as being from a surface with the position three temperature profile and of dimensions L_{eff} x W_{eff}. Therefore the effective length, L_{eff}, is 0.65 mm and the effective width, W_{eff}, is given by equation (7). These are the dimensions used in the theoretical section.

NEW SEMI-EMPIRICAL THEORY

The following analysis develops the relationship between wall shear stress and convection heat loss for a hot film gauge from the thermal energy integral equation :

$$\frac{d}{dx}\left[\int_0^\infty (T_b - T_\infty)\, U\, dy\right] = -\frac{dQ}{\rho\, C_p\, W_{eff}\, dx} \tag{8}$$

The theory is developed on the assumptions of steady incompressible flow over a one dimensional sensor. The heat transfer coefficient, pressure gradient, and the wall shear stress, are all assumed to be constant over the sensor effective length.

The approximation for the velocity distribution near the wall, for incompressible laminar flow, is derived from the solution of the momentum equation, with the assumption that in the region where the thermal boundary layer exists the inertia terms can be ignored. The implications of this assumption are covered by Menendez and Ramaprian (1985). The velocity distribution near the wall is then:

$$U = \frac{\tau_w}{\mu} y + \frac{1}{2\,\mu}\frac{dp}{dx} y^2 \tag{9}$$

Equations (8) and (9) can be manipulated to give:

$$\frac{d}{dx}\left[\tau_w \int_0^\infty y(T_b - T_\infty)\, dy + \frac{1}{2}\frac{dp}{dx}\int_0^\infty y^2 (T_b - T_\infty)\, dy\right] = -\frac{\mu^2\, dQ}{\rho\, K_f\, Pr\, W_{eff}\, dx} \tag{10}$$

To solve (10) an expression for the temperature distribution in the y direction is required which must satisfy the following boundary conditions:

$$\eta = 1 : T_b = T_\infty ; \frac{\partial T_b}{\partial y} = 0$$
$$\eta = 0 : T_b = T_x ; \frac{\partial T_b}{\partial y} = \frac{-dQ}{K_f\, W_{eff}\, dx} ; \frac{\partial^2 T_b}{\partial y^2} = 0 \tag{11}$$

The value T_x is the measured surface temperature distribution in the x direction over the sensor. Following Bellhouse and Schultz (1966) a fourth power temperature distribution is assumed. Evaluating the coefficients gives:

$$\frac{(T_b - T_\infty)}{(T_x - T_\infty)} = (1 - 4\eta^3 + 3\eta^4) + \lambda(\eta - 3\eta^3 + 2\eta^4) = f(\eta)$$
$$\text{Where : } \eta = \frac{y}{\delta_t} \quad ; \quad \lambda = \frac{-dQ\ \delta_t}{K_f\, W_{eff}\, dx\, (T_x - T_\infty)} \tag{12}$$

Substitution of (12) into (10) gives:

$$\int_{T_\infty}^{T_{max}} \left(\frac{2\,\tau_w\, K_f^2\, a}{h^2} - \frac{dp}{dx}\frac{K_f^3\, b}{h^3}\right) d[T_x - T_\infty] = -\int_0^{\frac{L_{eff}}{2}} \frac{2\,\mu^2\, h\, (T_x - T_\infty)\, dx}{\rho\, K_f\, Pr}$$
$$\text{Where } a = \lambda^2 \int_0^1 \eta f(\eta) d\eta = \lambda^2\left[\frac{1}{5} + \frac{\lambda}{15}\right]$$
$$b = \lambda^3 \int_0^1 \eta^2 f(\eta) d\eta = \lambda^3\left[\frac{2}{21} + \frac{\lambda}{28}\right] \tag{13}$$

The fluid properties are evaluated at the film temperature. As the sensor effective length is small, it is reasonable to assume that all terms except the surface temperature are constant in the flow direction. To perform the integrals of equation (13) all parameters except the surface temperature will be shown to be essentially constant in the flow direction.

For the gauge shown in Fig. 1 simple flat plate analysis gives only a 0.3% variation in the surface shear stress over the sensor, therefore τ_w in equation (13) is constant.

Conjugate analysis by Sugavanam *et al* (1994) has shown, for an isothermal heat source embedded in a large substrate, that as the ratio of thermal conductivities of the substrate to the fluid increases the streamwise variation in heat transfer coefficient over the thermally affected area becomes more uniform. In this case the sensor has a multilayered substrate consisting of kapton (polyimide) and aluminium which may be approximated as a single layer substrate by using orthotropic components of conductivity (Simeza and Yovanovich 1988). Series and parallel conductivity components, given in equation (14), represent the conductivities for the one dimensional heat flow through and in the plane of the substrate, respectively.

$$Series: \frac{H_{1,2}}{K_y} = \frac{H_1}{K_1} + \frac{H_2}{K_2} \quad \therefore K_y \approx 40.2 \ W/mK$$

$$Parallel: H_{1,2}K_x = K_1H_1 + K_2H_2 \quad \therefore K_x \approx 199.01 \ W/mK \tag{14}$$

The true value of conductivity would be between the series and parallel value. Using the worst case, the series approximation, gives a ratio of thermal conductivity of the substrate to the air of approximately 1675. The size of this ratio suggests that the heat transfer coefficient is essentially constant over the whole of the effective length of the sensor (Sugavanam *et al* 1994).

The values of parameters a and b, equation (15), are defined in terms of λ, which by inspection of equation (13) is seen to be dependent on the product of heat transfer coefficient and thermal boundary-layer thickness. For the values of a and b to be considered constant in the x direction, this product must also be constant. As the heat transfer coefficient and thermal boundary-layer thickness are inversely proportional to each other it would be reasonable to assume that the product of these values would also produce a constant value in the x direction.

For moderate values of free-stream pressure gradient, the gradient will not vary over the small sensor length.

Taking all these considerations into account equation (13) may be written as:

$$\frac{2\,\tau_w\,a\,K_f^2}{h^2}\int_{T_\infty}^{T_{max}} d[T_x-T_\infty] - \frac{dp}{dx}\frac{b\,K_f^3}{h^3}\int_{T_\infty}^{T_{max}} d[T_x-T_\infty] = -\frac{2\,\mu^2\,h}{\rho\,K_f\,Pr}\int_0^{\frac{L_{eff}}{2}}(T_x-T_\infty)dx \tag{15}$$

Using the empirical temperature distribution, equation (5), it can be shown:

$$2\int_0^{\frac{L_{eff}}{2}} W_{eff}\,h\,(T_x-T_\infty)dx = h\,W_{eff}\,L_{eff}\,(T_L-T_\infty) = Q_T \tag{16}$$

$$\therefore N_{u2} = \frac{Q_T}{K_f\,W_{eff}\,(T_L-T_\infty)} = \frac{(V_s^2 - V_0^2)}{R_h\,W_{eff}\,K_f\,(T_L-T_\infty)}$$

Using equations (16) equation (15) may be written as:

$$\left[\frac{\rho Pr}{\mu}\right]^{\frac{1}{3}} K_f\,W_{eff}\,2^{\frac{1}{3}}\,L_{eff}^{\frac{2}{3}}\,(T_L-T_\infty)^{\frac{2}{3}}\,(T_{max}-T_\infty)^{\frac{1}{3}}\cdot\left[a\,\tau_w - \frac{dp}{dx}\frac{b\,L_{eff}}{2\,N_{u2}}\right]^{\frac{1}{3}} = -\,Q_T \tag{17}$$

Equation (17) gives the relationship over the effective length of the sensor between the wall shear stress and the convective heat transfer.

The ohmic heating of the sensor is considered to be dissipated in two ways, convection to the free-stream fluid and conduction into the substrate which the sensor is mounted upon.

$$i_s^2R_h = -\,Q_T + i_0^2R_h \quad \therefore V_s^2 = -\,R_hQ_T + V_0^2 \tag{18}$$

Therefore:

$$\tau_w = \left[\frac{V_s^2 - V_0^2}{A'}\right]^3 + B'$$

Where :

$$A' = \left[\frac{\rho Pr}{\mu^2}\right]^{\frac{1}{3}} K_f\,R_h\,W_{eff}\,L_{eff}^{\frac{2}{3}}\,2^{\frac{1}{3}}(T_L-T_\infty)^{\frac{2}{3}}(T_{max}-T_\infty)^{\frac{1}{3}}\,a^{\frac{1}{3}}$$

$$B' = \frac{\frac{dp}{dx}\,b\,L_{eff}}{2\,a\,N_{u2}} \tag{19}$$

$$T_L = a_0 + \sum_{n=1}^{n=9}\frac{a_{2n-1}}{2n-1}\left(\frac{2}{\pi}\right)(-1)^{n+1}$$

DISCUSSION

The theory presented here is limited to one gauge and substrate type and to a restrictive set of flow conditions. What has been demonstrated, however, is that it is possible to derive a semi-empirical equation for these conditions, and, in the companion paper, Duffy *et al* (1995), it is shown that aerodynamic shear stress can be quantified on a turbine blade using this equation. By non-dimensionalising the final calibration equation (19), an equation can be derived that suggests that a gauge may be calibrated without knowledge of it's thermal dimensions. This approach would have to be verified experimentally, however, before it could be used.

The differences between the new and previous forms of the relationship between the wall shear stress and convective heat transfer can be seen by comparing equations (2) and (17). All sensor dimensions are now defined as effective sizes which are considered known. There are also new temperature parameters defining the mean and maximum temperature difference over the effective length of the sensor. Calibrating with this new equation will give different values of the calibration constants than those found by previous authors.

For the relationship of equation (18) to be correct the calibrating constants must not vary with Reynolds number. This has been verified experimentally. It is also supported by the fact that the temperature boundary-layer shape parameter, λ, is invariant with Reynolds number, Schlichting (1979), and that the calibrating constants are both functions of this parameter.

Integration of equation (12) gives a mean value for the shape parameter which can be used to give mean values of the calibration constants.

$$\overline{\lambda} = \frac{-Q_T\,\overline{\delta_t}}{K_f\,W_{eff}\,L_{eff}\,(T_L - T_\infty)}$$

$$\overline{a} = \overline{\lambda}^2\left[\frac{1}{5} + \frac{\overline{\lambda}}{15}\right] \quad ; \quad \overline{b} = \overline{\lambda}^3\left[\frac{2}{21} + \frac{\overline{\lambda}}{28}\right] \tag{20}$$

It may also be noted that because the sensor streamwise dimension is small, it is reasonable to assume that the shape parameter, λ, will not be a function of the surface geometry. Hence the theory may be applied to any shape of surface.

CONCLUSIONS

1) A new semi-empirical theory has been derived linking sensor voltage to aerodynamic shear stress.

2) Curve fitted temperature profiles have been used in the development of the new theory making the assumption of constant temperature over the sensor redundant.

3) The mean temperature over the sensor thermal area was found to remain constant to within ±1% with Reynolds number.

4) The accurate measurement of the sensor thermal area has enabled the calculation of more precise values of the effective dimensions than previously used.

5) The introduction of the effective width into the theory is a new concept as it takes into account the thermal effect on this dimension. This to some extent alleviates the assumption that the sensor is one dimensional.

6) Measured surface temperature profiles in the flow direction were found to be symmetric, indicating that the surface temperature is unaffected by the thermal boundary-layer growth.

7) This new information has also opened the way for the measurement of the two unknown calibrating parameters and therefore the measurement of aerodynamic wall shear stress with thin film gauges.

ACKNOWLEDGMENTS

The authors wish to acknowledge the financial support of the European Union and the University of Limerick. Also, the technical assistance of Mr. Paddy O'Donnell, Mr. John Griffin, and Mr. Paddy Kelly was much appreciated.

REFERENCES

Bellhouse, B. J., and Schultz, D. L., 1966, "Determination of Mean and Dynamic Skin Friction, Separation and Transition in Low-Speed Flow with a Thin-Film Heated Element," *Journal of Fluid Mechanics*, Vol. 24, Part 2, pp. 379-400.

Brown, G. L., 1967, "Theory and Application of Heated Films for Skin Friction Measurements," *Proceedings of 1967 Heat Transfer and Fluid Mechanics Institute*.

Curle, N., 1961, "Heat Transfer Through a Constant-Property Laminar Boundary-Layer Parts I and II," *Aeronautical Research Council*, R & M No. 3300.

Davis, M. R., 1980, "Design of Flat Plate Leading Edges to Avoid Flow Separation," *AIAA Journal*, Vol. 18, No. 5, pp 598-600.

Duffy, J. T., Davies, M. R. D., and Hamilton, L., 1995, "The Calibration of a Surface Mounted Aerodynamic Wall Shear Stress Gauge in Laminar Flow With a Free-Stream Pressure Gradient," to be presented at the 40Th ASME Gas Turbine and Aeroengine Congress, Exposition and Users Symposium, Houston, Texas, USA.

Hodson, H. P., 1985, "Boundary-Layer Transition and Separation Near the Leading Edge of a High-Speed Turbine Blade," ASME *Journal of Engineering for Gas Turbines and Power*, Vol. 107, pp 127-134.

Liepmann, H. W., 1958, "A Simple Derivation of Lighthill's Heat Transfer Formula," *Journal of Fluid Mechanics*, Vol. 3, Part 4, pp. 357-360.

Lomas, C., 1986, *Fundamentals of Hot Wire Anemometry*, Cambridge University Press.

Mathews, J., 1985, "The Theory and Application of Heated Films for the Measurement of Skin Friction," Ph.D. Thesis, Cranfield Institute Of Technology, Bedford, England.

Menendez, A. N., and Ramaprian, B. R., 1985, "The Use of Flush Mounted Hot Film Gauges to Measure Skin Friction in Unsteady Boundary-Layers," *Journal of Fluid Mechanics.*, Vol. 161, pp. 139-159.

Pope, R. J., 1972, "Skin Friction Measurements in Laminar and Turbulent Flows Using Heated Thin Film Gauges," *AIAA Journal*, Vol. 10, No. 6, pp. 729-730.

Schroeder, Th., 1989, "Measurements With Hot-Film Probes and Surface Mounted Hot-Film Gauges in a Multistage Low-Pressure Turbine," Report for European Propulsion Forum, pp 15.1-15.27.

Schlichting, H.,1979, *Boundary-Layer Theory*, Seventh Edition, Mc-Graw Hill, New York.

Simeza, L. M., and Yovanovich, M. M., 1988, "Thermal Analysis of Multilayered Printed Circuit Boards Using a Hybrid Integral-Thermal Network Method," *Proceedings of the 20th International Symposium on Heat Transfer in Electronic and Microelectronic Equipment*, Dubrovnik, Yugoslavia.

Sugavanam, R., Ortega, A., and Choi, C. Y., 1994, "A Numerical Investigation of Conjugate Heat Transfer From a Flush Heat Source on a Conductive Board in Laminar Channel Flow," *Proceedings of the 4th I-Therm Intersociety Conference on Thermal Phenomena In Electronic Systems*, pp. 62-72, Washington DC, USA.